International Journal for Parasitology 47 (2017) 811–821

Contents lists available at ScienceDirect

International Journal for Parasitology

journal homepage: www.elsevier.com/locate/ijpara

In vitro efficacy of bumped kinase inhibitors against *Besnoitia besnoiti* tachyzoites

Alejandro Jiménez-Meléndez [a], Kayode K. Ojo [b], Alexandra M. Wallace [b], Tess R. Smith [b], Andrew Hemphill [c], Vreni Balmer [c], Javier Regidor-Cerrillo [a], Luis M. Ortega-Mora [a], Adrian B. Hehl [d], Erkang Fan [e], Dustin J. Maly [e,f], Wesley C. Van Voorhis [b], Gema Álvarez-García [a,*]

[a] SALUVET, Animal Health Department, Faculty of Veterinary Sciences, Complutense University of Madrid, Ciudad Universitaria s/n, 28040 Madrid, Spain
[b] Center for Emerging and Re-emerging Infectious Diseases (CERID), Division of Allergy and Infectious Diseases, Department of Medicine, University of Washington, Seattle, WA, USA
[c] Institute of Parasitology, Vetsuisse Faculty, University of Berne, Länggass-Strasse 122, CH-3012 Berne, Switzerland
[d] Institute of Parasitology, University of Zurich, Winterthurerstrasse 266a, Zurich CH-8057, Switzerland
[e] Department of Biochemistry, University of Washington, Seattle, WA 98195-7742, USA
[f] Department of Chemistry, University of Washington, Seattle, WA 98195-1700, USA

ARTICLE INFO

Article history:
Received 27 April 2017
Received in revised form 25 August 2017
Accepted 29 August 2017
Available online 9 September 2017

Keywords:
Besnoitia besnoiti
Chemotherapy
Bumped kinase inhibitors
CDPK1
In vitro assay

ABSTRACT

Besnoitia besnoiti is an apicomplexan parasite responsible for bovine besnoitiosis, a chronic and debilitating disease that causes systemic and skin manifestations and sterility in bulls. Neither treatments nor vaccines are currently available. In the search for therapeutic candidates, calcium-dependent protein kinases have arisen as promising drug targets in other apicomplexans (e.g. *Neospora caninum*, *Toxoplasma gondii*, *Plasmodium* spp. and *Eimeria* spp.) and are effectively targeted by bumped kinase inhibitors. In this study, we identified and cloned the gene coding for *Bb*CDPK1. The impact of a library of nine bumped kinase inhibitor analogues on the activity of recombinant *Bb*CDPK1 was assessed by luciferase assay. Afterwards, those were further screened for efficacy against *Besnoitiabesnoiti* tachyzoites grown in Marc-145 cells. Primary tests at 5 μM revealed that eight compounds exhibited more than 90% inhibition of invasion and proliferation. The compounds BKI 1294, 1517, 1553 and 1571 were further characterised, and EC_{99} (1294: 2.38 μM; 1517: 2.20 μM; 1553: 3.34 μM; 1571: 2.78 μM) were determined by quantitative real-time polymerase chain reaction in 3-day proliferation assays. Exposure of infected cultures with EC_{99} concentrations of these drugs for up to 48 h was not parasiticidal. The lack of parasiticidal action was confirmed by transmission electron microscopy, which showed that bumped kinase inhibitor treatment interfered with cell cycle regulation and non-disjunction of tachyzoites, resulting in the formation of large multi-nucleated complexes which co-existed with viable parasites within the parasitophorous vacuole. However, it is possible that, in the face of an active immune response, parasite clearance may occur. In summary, bumped kinase inhibitors may be effective drug candidates to control *Besnoitiabesnoiti* infection. Further in vivo experiments should be planned, as attainment and maintenance of therapeutic blood plasma levels in calves, without toxicity, has been demonstrated for BKIs 1294, 1517 and 1553.

© 2017 Australian Society for Parasitology. Published by Elsevier Ltd. All rights reserved.

1. Introduction

Besnoitia besnoiti is an apicomplexan parasite responsible for bovine besnoitiosis, a chronic and debilitating disease of cattle that causes systemic and skin manifestations, as well as sterility in bulls. At present, it is considered a re-emerging cattle disease in Europe. It has spread towards northern and central eastern Europe, given the absence of effective treatments or vaccines and the lack of common policies concerning animal trade (European Food Safety Authority, 2010; Álvarez-García et al., 2013; Álvarez-García, 2016).

Taxonomically, *B. besnoiti* belongs to the subfamily Toxoplasmatinae, together with other cyst-forming parasites of veterinary and human health importance, such as *Neospora caninum* and *Toxoplasma gondii*, respectively. Similarly, it has a heteroxenous life cycle but the definitive host has not yet been identified (Diesing et al., 1988; Basso et al., 2011). Domestic bovines and wild ruminants such as antelopes and roe deer (Arnal et al., 2017) act as

* Corresponding author.
E-mail address: gemaga@ucm.es (G. Álvarez-García).

http://dx.doi.org/10.1016/j.ijpara.2017.08.005
0020-7519/© 2017 Australian Society for Parasitology. Published by Elsevier Ltd. All rights reserved.

intermediate hosts, where two asexual infective stages of the parasite develop: initially, fast-replicating tachyzoites are found inside endothelial cells of blood vessels during the acute stage of the disease, which may go unnoticed due to the non-specific clinical signs such as fever, anorexia or swelling of lymph nodes (reviewed by Álvarez-García et al., 2014). During the chronic stage of the disease, when the immune response is elicited against the parasite, tachyzoites switch into slowly dividing bradyzoites. Bradyzoites form tissue cysts are located mainly in the subcutaneous (s.c.) connective tissue and are responsible for the characteristic lesions found during the chronic stage.

In bovines, treatments attempted for besnoitiosis have included the use of formalin, sulphametazine, toltrazuril or oxytetracycline (Franc and Cardiegues, 1999). In laboratory settings, experimentally infected rabbits were treated with formalin, pentamidines, sulphonamides, trimethoprim, pyrimethamine and oxytetracycline (Pols, 1960; Shkap et al., 1985, 1987) and oxytetracycline was applied in gerbils (Shkap et al., 1985). Unfortunately, all these studies had been carried out under very different experimental conditions with a limited number of animals, and results were mainly based on clinical inspection and histopathology. In vitro studies showed that arylimidamides (Cortes et al., 2011) and thiazolides (Cortes et al., 2007) have activity against *B. besnoiti*, but further research with well-established and reliable experimental models, both in vitro and in vivo, is urgently needed.

Apicomplexan calcium-dependent protein kinases (CDPKs) belong to a superfamily of serine-threonine kinases. They are conserved enzymes among members of the phylum Apicomplexa, but are absent in mammalian cells (Ward et al., 2004; Srinivasan and Krupa, 2005; Billker et al., 2009). CDPKs thus represent parasite-specific drug targets. Bumped kinase inhibitors (BKIs), namely pyrazolo-pyrimidine and 5-aminopyrazole-4-carbomidecarboxa mide analogues, specifically designed to act on CDPK1 (Lourido and Moreno, 2015; Van Voorhis et al., 2017) have shown efficacy against *T. gondii* (Ojo et al., 2010; Doggett et al., 2014); *N. caninum* (Ojo et al., 2014; Winzer et al., 2015); *Babesia* spp. (Pedroni et al., 2016), *Cryptosporidium parvum* (Lendner et al., 2015) and *Plasmodium* spp. (Ojo et al., 2012; Van Voorhis et al., 2017). In *T. gondii,* CDPK1 plays a crucial role in gliding motility, microneme secretion, host cell invasion and egress, and parasite differentiation by means of calcium-dependent mechanisms (Lourido et al., 2010; Lourido and Moreno, 2015). Bumped kinase inhibitors (Doerig et al., 2002; Greenbaum, 2008) selectively bind to a hydrophobic pocket adjacent to the ATP binding site. This hydrophobic pocket is made accessible by a small "gatekeeper" amino-acid such as glycine, a unique characteristic of some apicomplexan CDPK1 s. Pharmacological inhibition of either *Tg*CDPK1 or *Nc*CDPK1 with BKIs in vitro blocks host cell invasion, thereby inhibiting parasitic growth (Ojo et al., 2010; Winzer et al., 2015).

Currently, the exact mechanisms of host cell invasion and proliferation of *B. besnoiti* are not well understood, but Frey et al. (2016) demonstrated that lytic cycle events are similar to those exploited by closely related *N. caninum* and *T. gondii*. *Besnoitia besnoiti* CDPK1 has not yet been identified. However, the existence of the orthologue *Bb*CDPK1 is likely since it has been proven that members of the Toxoplasmatinae share a high degree of homology in relation to CDPK enzymes (Keyloun et al., 2014; Ojo et al., 2014). Recently, a standardised experimental in vitro model of infection using an epithelial-like cell line (Frey et al., 2016) was developed. This model allowed a detailed study of the *B. besnoiti* lytic cycle, revealing that these parasites can survive extracellularly for extended periods of time (up to 24 h p.i.), and showed that *Besnoitia* tachyzoites generally have a low invasion rate and proliferate asynchronously. The establishment of this in vitro model set the basis for performance of drug screening and testing of potential therapeutic candidates against this protozoal agent.

The rational approach followed herein has been previously exploited in the closely related protozoans *T. gondii* and *N. caninum*, where CDPK orthologues were identified and a variety of compounds were screened in in vitro assays (Van Voorhis et al., 2017). Thus, in the present study, we identified and characterised *Bb*CDPK1 and evaluated the efficacy of nine BKIs against *B. besnoiti* tachyzoites in a standardized in vitro assay model.

2. Materials and methods

2.1. Parasite maintenance and cell cultures

Marc-145 and Human Foreskin Fibroblast (HFF) cells were maintained in DMEM (Gibco, Thermo Fisher Scientific, Waltham, MA, USA) with phenol red supplemented with 10% heat inactivated and sterile filtrated faetal calf serum (FCS) (Gibco, Thermo Fisher Scientific, Waltham, MA, USA), 5 mM HEPES (pH 7.2), 2 mM glutamine (Lonza Group, Basel, Switzerland), and a mixture of penicillin (100 U/ml), streptomycin (100 µg/ml) and amphotericin B (Lonza Group, Basel, Switzerland) as previously published (Frey et al., 2016). They were cultured at 37 °C and 5% CO_2 in 75 or 25 cm^2 tissue culture flasks. Marc-145 cell cultures were passaged twice each week, HFFs once each week. *Besnoitia besnoiti* Spain1 (Bb-Spain1) used for all in vitro assays and Evora (Bb-Evora) strains were maintained by serial passages in Marc-145 cells in the same culture medium with 5% FCS (Fernández-García et al., 2009a). FCS used in all the experiments was previously checked for the absence of specific IgG against *B. besnoiti*, *N. caninum* and *T. gondii* by IFAT (Fernández-García et al., 2009b).

Tachyzoites were harvested 3 days p.i., when the majority of them were still intracellular, by recovering the infected cell monolayer with a rubber cell scraper, followed by repeated passages through a 25 gauge needle at 4 °C and separation from cell debris on a PD-10 column (GE Healthcare, Little Chalfont, United Kingdom) (Frey et al., 2016). Tachyzoite viability was confirmed by trypan blue exclusion followed by counting in a Neubauer chamber. Purified tachyzoites were used to infect Marc-145 or HFF cell monolayers as described in Section 2.5.1.

2.2. BbCDPK1 identification, sequencing and cloning

2.2.1. NCBI BLAST® search and Clustal analyses

The amino acid sequence of *Nc*CDPK1 (NCLIV_011980) from ToxoDB (www.toxodb.org) was used in order to retrieve orthologous genes in apicomplexan parasites using the NCBI BLAST® tool (https://blast.ncbi.nlm.nih.gov/Blast.cgi). Nucleotide sequences coding for related sequences of CDPK1 in *T. gondii*, *N. caninum* and *Hammondia hammondi* were considered (Supplementary Fig. S1). Clustal Omega (http://www.ebi.ac.uk/Tools/msa/clustalo/) was employed to align nucleotide and protein sequences. Next, three pairs of primers (Table 1) were designed in conserved, homologous regions (BbCDPK1Fw2; BbCDPK1Fw3, BbCDPK1Rv1 and BbCDPK1FwC) (Supplementary Fig. S1).

Total RNA from the Bb-Evora strain collected from infected Marc-145 monolayers at 8 h p.i. was stored in RNA later reagent (Qiagen, Valencia, CA, USA) and cDNA was synthetized using a SuperScript Vilo® cDNA synthesis kit (Life technologies, Thermo Fisher Scientific, Waltham, MA, USA) according to the manufacturer's instructions. cDNA was diluted 1:10 in molecular grade distiled H_2O. cDNA from the Nc-Liverpool strain of *N. caninum* was also employed to test specificity of the primers used.

polymerase chain reaction (PCR) conditions were 94 °C for 5 min, 35 cycles at 94 °C for 30 s, 60 °C for 1 min and 72 °C for 1 min 30 s and a final elongation at 72 °C for 10 min. PCRs were carried out with the Platinum® Taq DNA Polymerase High Fidelity

Table 1
List of primers used in the present study.

Use	Primer sequence (5′–3′)
Protein identification and sequencing	FW2: GAAGCAGAAGACGGACAAGGAGTC FW3: GCATCATCGACTTTGGCCTCAGCA FWC: GACGAGCTCCACGCGACGCCGGGGATGTTCGTT RV1: GGT TAA TTA ATT TCC GCA GAG CTT CAA GAG CAT
Protein cloning	Bb_LIC_Fw: GGG TCC TGG TTC GAT GGG TCA GCA AGA AAG CAC GCT CGG C Bb_LIC_Rev: CTT GTT CGT GCT GTT TAC TTA GTT GCC GCA GAG CTT CAG AAG

(Invitrogen, Thermo Fisher Scientific, Waltham, MA, USA) and all primers were purchased from Sigma–Aldrich. PCR products were visualised in 1.5% agarose gel stained with ethidium bromide and next purified using the Geneclean Turbo® kit (QBiogene, Montreal, Canada) according to the manufacturer's instructions for sequencing. PCR products were directly sequenced in both directions using the Big Dye® Terminator v3.1 Cycle Sequencing Kit (Applied Biosystems, Thermo Fisher Scientific, Waltham, MA, USA) and a 3730 DNA analyser (Applied Biosystems, Thermo Fisher Scientific, Waltham, MA, USA) at the Unidad Genómica del Parque Científico de Madrid, Spain. Sequence data were analysed using BioEdit Sequence Alignment Editor v.7.0.1 (Hall, 1999) (Copyright_ 1997–2004 Tom Hall, Ibis Therapeutics, Carlsbad, CA, USA).

The sequence obtained (see Section 3.1) was compared with the *B. besnoiti* genome (the genome sequence is the property of the University of Zurich, Switzerland and will be made freely available to the community on NCBI and EuPathDB after publication). After retrieving the coding sequence using the GeneWise-Pairwise Sequence Alignment (EMBL-EBI) tool in order to process introns, a truncated region of the Bb*CDPK1* gene was amplified from *B. besnoiti* Evora strain cDNA using primers Bb_LIC_Fw (5′-GGG TCC TGG TTC GAT GGG TCA GCA AGA AAG CAC GCT CGG C-3′) and Bb_LIC_Rev (CTT GTT CGT GCT GTT TAC TTA GTT GCC GCA GAG CTT CAG AAG-3′) (data not shown). The PCR product was cloned into the ligation-independent cloning (LIC) site of expression vector pAVA0421 and expressed and purified as previously published for *Nc*CDPK1 (Ojo et al., 2014). The purified protein was visualised by SDS–PAGE and Coomassie staining (Supplementary Fig. S2).

2.2.2. In silico analysis and prediction of N-myristoylation and palmitoylation

The predicted molecular weight of *Bb*CDPK1 was obtained using ExPasy tools for prediction of protein properties (ProtParam; http://web.expasy.org/protparam). The Simple Modular Architecture Research Tool (SMART; http://smart.embl-heidelberg.de) was used to predict functional domains in proteins. Myristoylation prediction was carried out using Prosite PDOC00008 (http://www.expasy.ch/prosite/) as described by Etzold et al. (2014) for CDPKs from *C. parvum*. Palmitoylation sites were predicted with CSS-Palm 2.0 (http://csspalm.biocuckoo.org).

Modelling of *Bb*CDPK1 secondary and tertiary structures was performed using the I-TASSER online tool (http://zhanglab.ccmb.med.umich.edu) (Yang et al., 2015).

2.3. BbCDPK1 enzymatic activity assays and its inhibition by BKIs

Protein kinase activity of recombinant *Bb*CDPK1 (r*Bb*CDPK1) and inhibition of its kinase phosphorylation properties by a panel of BKIs (Keyloun et al., 2014) was measured in a non-radioactive assay using Kinase-Glo® luciferase reagent (Promega, Madison, WI, USA) as previously described (Ojo et al., 2014). Basically, this luminescence-based assay measures kinase activity in the presence or absence of inhibitors by reporting changes in initial ATP concentrations. Kinase phosphorylation reactions were performed as previously published for *Nc*CDPK1 (Ojo et al., 2014) in a 25 μL buffered solution containing 20 mM HEPES (pH, 7.5), 0.1% BSA, 10 mM $MgCl_2$, 1 mM EGTA, 2 mM $CaCl_2$, 20 μM peptide substrate (Biotin-C6-PLARTLSVAGLPGKK) (BioSyntide-2) (American Peptide Company, Inc. Sunnyvale, CA, USA), 3.5 nM *Bb*CDPK1, and 2 to 0.00012207 μM inhibitor (4-fold serial dilutions). Phosphorylation reactions were initiated by the addition of 10 μM Na_2ATP (Sigma–Aldrich, St. Louis, MO, USA). After incubating for 90 min at 30 °C, the reaction was terminated by adding EGTA to a final concentration of 5 mM. Changes in the initial ATP concentration were evaluated as a luminescence readout using a MicroBeta2 multilabel plate reader (Perkin Elmer, Waltham, MA, USA). Results were converted to percent inhibition and IC_{50} values (the concentration of compound that led to 50% inhibition of enzyme activity) using non-linear regression analysis in GraphPad Prism (GraphPad Software, La Jolla, CA, USA).

2.4. Mammalian cell toxicity assays

The potential toxicity of the compounds against a mammalian cell line was determined by an XTT cell viability assay (Panreac Applichem, Darmstadt, Germany) to quantify cell growth. Marc-145 cells in the exponential phase of growth were seeded in 96-well flat-bottomed plates at a density of 2×10^5 cells/mL containing compounds (20 mM stock solutions dissolved in dimethyl sulfoxide (DMSO) at the maximum concentration employed in our assays (5 μM) in quadruplicate and grown for 72 h at 37 °C in a 5% CO_2 humidified incubator. Afterwards, 50 μL of XTT reagent was added to each well and incubated for 4 h. Fluorescence was measured at the respective excitation and emission wavelengths of 475 nm and 660 nm in a Synergy™ H1 microplate reader (Biotek Instruments Inc, Winooski, VT, USA). The percentage of growth inhibition was computed for any BKI tested, based on the DMSO vehicle. Three independent assays were performed with nine selected BKIs employed in the screening assays.

2.5. In vitro drug efficacy

Nine BKIs previously optimised with functional groups for improved potency, selectivity and pharmacokinetic properties were selected for further studies (Supplementary Fig. S3). The purity of all compounds (>98%) was confirmed by reverse-phase HPLC and ^{1}H-Nuclear Magnetic Resonance (NMR). (Doggett et al., 2014; Ojo et al., 2014, 2016; Huang et al., 2015; Vidadala et al., 2016). BKIs were sent to Saluvet research group (Complutense University of Madrid, Spain) at a concentration of 20 mM diluted in 100% DMSO. Compounds were stored, protected from light, at -20 °C.

2.5.1. Drug screening

Marc-145 cells (5×10^4 cells per well) were incubated in culture media at 37 °C with 5% CO_2 and grown to confluence in 24-well plates. In the initial drug screening, inhibitors were added at a final concentration of 5 μM, just prior to infection with purified tachyzoites from the Bb-Spain1 strain. DMSO (as solvent) was added to negative control wells at the same final concentration. Cultures were subsequently infected with 10^3 purified tachyzoites from the Bb-Spain1 strain. Another set of experiments adding the different compounds 6 h p.i., when 50% invasion rate is reached for the strain employed (Frey et al., 2016), was also performed to address possible effects on parasite proliferation. Before

administration of the compounds, infected monolayers were gently rinsed with PBS three times in order to discard non-invaded tachyzoites. In both sets of experiments, immunofluorescence assays were performed after 3 days at 37 °C/5% CO_2 (see Section 2.6) to count invasion events per well. Each condition was assessed in triplicate and the experiments were carried out in three independent assays. Those compounds that showed the highest values of both parasite invasion and proliferation inhibition were selected for further experiments.

2.5.2. Short-term assays: EC_{50} and EC_{99} determination

Marc-145 cells were grown as mentioned above in 24 well plates. Just prior to infection, BKIs were added at final concentrations ranging from 5 nM to 5 μM for determination of EC_{50} and EC_{99} (the effective concentration to reduce parasite numbers 50% or 99%, respectively) values. Then, Bb-Spain1 tachyzoites were added at a parasite:host cell ratio of 1:100 (10^3 tachyzoites per well). DMSO control wells were also included in each culture plate.

A similar experiment to determine the effects of the compounds on *B. besnoiti* proliferation was also performed. Here, infection of host cell monolayers was performed as previously described and compounds 1294, 1517, 1553 or 1571 were added at a final concentration from 5 nM to 5 μM per well at 24 h p.i., when the parasite invasion is completed (Frey et al., 2016). Prior to the addition of the compounds, three washes with PBS were performed in order to discard non-invaded tachyzoites.

After 72 h p.i., samples were collected using a lysis solution (100 μL of PBS, proteinase K and AL Buffer) according to the manufacturer's instructions contained in the DNeasy® Blood and Tissue kit (Qiagen, Valencia, CA, USA), for further DNA extraction and quantitative real-time (qPCR) to quantify the number of parasites in each well. Immunofluorescence staining was also performed as stated below for each compound and concentration used at 72 days p.i. Each condition was assessed in triplicate and the experiments were carried out in three independent assays.

2.5.3. Characterisation of long-term effects of BKI treatments on B. besnoiti tachyzoites

Tachyzoites from the Bb-Spain1 strain were grown as previously stated and compounds 1294 1517, 1553 and 1571 were added just prior to infection at the previously established EC_{99} concentration. Drugs were left in the cultures for 6, 24 or 48 h. Drugs containing media were discarded and fresh culture media were added. Samples were collected at 1, 3 and 5 days post treatment for subsequent qPCR analysis. IFAT was performed at 8 and 10 days post treatment to assess whether any tachyzoites were able to re-infect host cells (Winzer et al., 2015). Each condition was assessed in triplicate and the experiments were carried out in three independent assays.

2.5.4. Transmission Electron Microscopy analysis of B. besnoiti – infected HFFs treated with selected BKIs

HFF cell cultures were maintained in T25 tissue culture flasks and were infected with 10^7 Bb-Spain1 tachyzoites (parasite:host cell ratio of 10:1). After allowing the tachyzoites to invade the host cells for 3 h, monolayers were washed three times with PBS and treated with BKIs at a concentration of 5 μM. Samples were processed for Transmission Electron Microscopy (TEM) analysis at different time points after infection (4, 6 and 8 days) as described earlier (Winzer et al., 2015; Müller et al., 2017).

2.6. Immunofluorescence staining

For immunofluorescence staining, supernatants of the cell cultures were discarded at 72 h p.i., wells were washed three times with PBS and subsequently fixated with ice-cold methanol or paraformaldehyde 3%- glutaraldehyde 0.05% for 10 min. Then, wells were washed a further three times with PBS. Afterwards, those were incubated with 300 μL/well of Triton-X 100 (0.2%) in PBS for 30 min at 37 °C, followed by three additional washes with PBS. As primary antibody, a polyclonal rabbit-anti tachyzoite Bb-Spain1 (Gutiérrez-Expósito et al., 2013) was added at a dilution of 1:1000 in PBS and incubated for 1 h at 37 °C. After three additional washes with PBS, 250 μL of Alexa Fluor® 488 Goat Anti-Rabbit IgG (H + L) (Life technologies, Carlsbad, CA, USA) were added per well at a dilution of 1:1000. The plates were incubated for 45 min at room temperature in the darkness and washed three times with PBS. In the final wash, DAPI stain was included. Finally, the plates were washed with distiled water and the total number of invasion events per well was counted using an inverted fluorescence microscope (Nikon Eclipse TE200) at 200× magnification. Two categories of plaque forming tachyzoites were distinguished: parasitophorous vacuoles (PVs) and lysis plaques, as described by Frey et al. (2016). For the isolate employed, 80% of the invasion events consisted of lysis plaques at 72 h p.i.

2.7. DNA extraction and quantitative real-time PCR (qPCR)

The harvested cell culture samples were incubated for 10 min at 56°C. Afterwards, DNA was purified using the spin column protocol for cultured cells according to the manufacturer's instructions contained in the DNeasy®Blood and Tissue kit (Qiagen, Valencia, CA, USA). DNA was eluted in 200 μL of elution buffer. The DNA content and purity of each sample was measured by UV spectrometry (Nanophotometer®, Implen GmbH, Munich, Germany).

The BbRT2 qPCR assay for specific detection of *Besnoitia* spp. DNA from ungulates (i.e., *B. besnoiti*, *Besnoitia tarandi, Besnoitia caprae* and *Besnoitia bennetti*) was performed according to Frey et al. (2016). Briefly, each 20 μL reaction contained 10 μl of Power SYBR Green master mix® (Applied Biosystems, Thermo Fisher Scientific, Foster City, CA, USA), 0.5 μl of primer Bb3 (5′-CAA CAA GAG CAT CGC CTT C-3′; 20 μM), 0.5 μl of primer Bb 6 (5′-ATT AAC CAA TCC GTG ATA GCA G-3′; 20 μM), and 4 μl of water. The qPCRs were run on a 7300 Real-Time PCR System® (Applied Biosystems). Twenty to 100 ng of DNA in a volume of 5 μl was added to each reaction. The DNA positive control was extracted from *B. besnoiti* tachyzoites cultured in vitro. The product of the DNA extraction process using water instead of cells was used as a negative control. In each qPCR, 10-fold serial dilutions of genomic DNA corresponding to 0.1–100,000 Bb-Spain1 tachyzoites were included. The cycling conditions were 10 min at 95 °C followed by 40 cycles of 95 °C for 15 s and 60 °C for 1 min. Fluorescence emission was measured during the 60 °C step. A dissociation stage was added at the end of each run, and the melting curves were analysed. BbRT2-PCR was run in duplicate for each sample. The threshold cycle values (Ct-values) obtained for positive samples in the BbRT2-PCR were also expressed as tachyzoites per reaction using the standard curve included in each run.

2.8. Data analyses

The cytotoxicity of screened BKIs was compared by a one-way ANOVA test. For the determination of the percentage of inhibition (%) in the in vitro drug screening, first the invasion rate (IR) was calculated by counting all the events per well. Then, invasion rates were related to the negative control (DMSO) to determine the relative invasion rate (RIR) of the parasite for each condition. Afterwards, the% of inhibition was determined as indicated below.

$$\%\text{RIR} = (\text{IR treated well}/\text{IR DMSO well}) \times 100$$

$$\%\text{Inhibition} = 100 - \%\text{RIR}$$

For the compounds that showed the highest percentages of inhibition in the initial drug screening at 0 and 6 h p.i., tachyzoite yields after 72 h of incubation were determined by qPCR for EC_{50} and EC_{99} calculations, and adjusted to the amount of DNA quantified by spectrophotometry in each sample. The relative growth for each drug concentration was determined relative to the DMSO control, using the tachyzoite yield per ng of DNA. Afterwards, the EC_{50} and EC_{99} concentrations were determined using an ED_{50} plus sheet for Microsoft Excel after a logarithmic transformation of the data.

The Kruskal–Wallis test was performed to compare the efficacy of the nine compounds against *B. besnoiti* in the drug screening, and to search for differences among the four compounds selected for determination of EC_{50} and EC_{99} values. This test was also used to address whether there were differences among the different concentrations of BKIs tested. Finally, a two-way ANOVA test was employed to compare the different treatment durations employed. All statistical analyses were performed using the software GraphPad Prism® 6.0 (GraphPad Software, San Diego, CA, USA). For all statistical analyses, $P < 0.05$ was considered significant.

3. Results

3.1. BbCDPK1 identification, sequencing and cloning

The partial sequence of *Bb*CDPK1 initially obtained consisted of a 1160 bp sequence that showed features characteristic of a CDPK1 enzyme, including the amino-acid sequence of the putative active site of the enzyme, which was identical to the one present in *Nc*CDPK1 (Fig. 1). When the whole sequence data were subjected to intron processing, the complete coding sequence obtained showed 95% identity both in nucleotide and amino acid sequences compared with *Nc*CDPK1 and *Tg*CDPK1 sequences, including the putative active site with a glycine gatekeeper (Fig. 1; GenBank® accession number N° **KY991370**). The expected molecular weight of the obtained protein was 56 kDa (Expasy ProtParam). Using the Simple Modular Architecture Research Tool (EMBLEM, Heidelberg, Germany) for protein sequence analysis and classification, the sequence obtained showed a kinase domain with an ATP binding site and four EF hand domains for calcium binding, as described for other apicomplexan CDPK1 enzymes (Fig. 1). Moreover, putative sites of N-mirystoilation were found in the N-terminal region of the protein, as well as one site of palmytoilation. *Bb*CDPK1 showed 98 and 98.4% amino acid identity in the kinase domain with *Tg*CDPK1 and *Nc*CDPK1, respectively.

Not surprisingly, results from I-TASSER modelling showed that *Tg*CDPK1 has the closest structural similarity.

3.2. Screening of recombinant BbCDPK1 using BKI-analogues

Due to the close homology of *Bb*CDPK1 with CDPK1 in other apicomplexans, the enzyme was expressed as a recombinant protein to test the effects of BKI analogues on its activity. Upon separation by SDS–PAGE, recombinant *Bb*CDPK1 exhibited a molecular weight of 57 kDa (Fig. 1). Nine BKIs, namely BKI-1294, 1605, 1649, 1517, 1553, 1571, 1575, 1586 and 1597, inhibited *Bb*CDPK1 with IC_{50} values in the lower nanomolar range (Table 2). Thus, these compounds were further assessed in cellular assays. The activity of the recombinant enzyme was proven to be calcium-dependent, so it is highly unlikely that the activity was not associated with the recombinant enzyme itself.

3.3. Cytotoxicity in Marc-145 cells

When the compounds were added to uninfected Marc-145 cells at the highest concentration employed in the in vitro assays

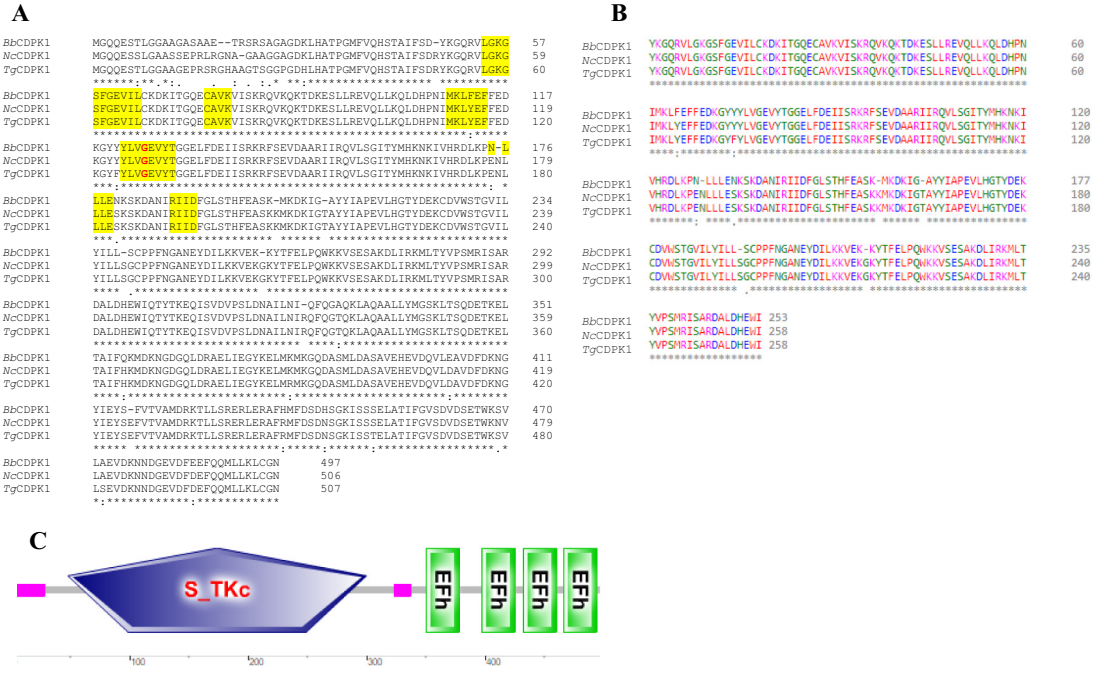

Fig. 1. Sequence features of *Bb*CDPK1 (GenBank® accession number **KY991370**). (A) Alignment of amino acids sequences of *Bb*CDPK1, *Nc*CDPK1 and *Tg*CDPK1. Yyellow highlighted amino acids were postulated by Keyloun et al. (2014) to contribute to the potential activity or resistance of CDPK1 enzymes to bumped kinase inhibitors. Gatekeeper (Gly) is marked in red. (B) Alignment of amino acid sequences of the kinase domain of *Bb*CDPK1, *Nc*CDPK1 and *Tg*CDPK1. (C) Simple Modular Architecture Research Tool (SMART) image of *Bb*CDPK1, with the serin-threonin kinase domain and four calcium-binding EF hands. *Bb*, *Besnoitia Besnoiti*, *Nc*, *Neospora caninum*, *Tg*, *Toxoplasma gondii*.

Table 2
Activity of bumped kinase inhibitors screened against *Besnoitia besnoiti* CDPK1 activity (IC_{50} values (μM)).

Compound	1294	1517	1553	1571	1575	1586	1597	1605	1649
IC_{50} (r*Bb*CDPK1)	0.004	0.012	0.004	0.024	0.022	0.011	0.002	0.015	0.006

(5 μM), those did not cause significant cytotoxicity compared with DMSO ($P > 0.05$; one-way ANOVA). Percentages of cytotoxicity of the screened BKIs compared with the DMSO-treated negative control wells were as follows: 1294: 5.2%; 1517: 5.2%; 1553: 5.8%; 1571: 2.8%; 1575: 4%; 1586: 5%; 1597: 5.1%; 1605: 3.8%; 1649:5%. Moreover, upon inspection by light microscopy, no alterations in the Marc-145 cell morphology were detected.

3.4. Initial drug screening of BKIs in B. besnoiti-infected Marc-145 cells

In the initial drug treatments carried out at the time point of infection (0 h p.i.) and 6 h p.i., eight out of nine BKIs caused more than 80% of parasite growth inhibition. Compound 1649 was the least effective (63%, Kruskal–Wallis test, $P < 0.01$), whereas 1294, 1517, 1553 and 1571 were the most efficacious, and were thus selected for further studies (Table 3). Parasite growth was markedly inhibited in drug-treated wells since only parasitophorous vacuoles (PVs) were found, whilst in DMSO-treated control wells parasites were displaying the normal features of their lytic cycle at 72 h p.i. as a consequence of parasite egress (Frey et al., 2016), where most invasion events consisted of plaques lysis.

3.5. Dose–response experiments and EC_{50} and EC_{99} determination

All four selected BKIs led to a significant reduction in parasite growth when administered at concentrations higher than 0.05 μM at the time point of infection (Fig. 2A). When BKIs were added at 5 μM at 24 h p.i., parasite proliferation was still inhibited by 80%, indicating that these compounds inhibit both host cell invasion and intracellular proliferation (Fig. 2B). The EC_{50} and EC_{99} values determined at 0 h p.i. were largely in a similar range among these compounds, except for 1553, which appeared slightly less efficacious (Table 4). Treatments with compounds 1294 and 1517 showed the lowest parasite loads. Statistically significant differences in the number of parasites per well were found between compounds 1517 and 1571 at a concentration of 5 μM when administered at 0 h p.i. (Kruskal–Wallis, $P < 0.05$), and among the different concentrations for each BKI (Kruskal–Wallis, $P < 0.01$).

3.6. Characterisation of the long-term post-treatment effects of BKI exposure on B. besnoiti tachyzoites

Following BKI treatments for various time spans, parasite growth was hardly detected until 3 days p.i., and statistically significant differences between the four BKI-treated and DMSO-treated cultures were observed at 5 days post treatment for each of the treatment durations ($P < 0.001$, two-way ANOVA) (Fig. 3). Differences were also found among the different treatment durations (6, 24 and 48 h) for each BKI ($P < 0.001$, two-way ANOVA) (Fig. 3). Upon short treatments (6 h) with the four BKIs, compounds 1553 and 1517 showed statistically significant differences ($P < 0.01$, two-way ANOVA), and the lowest tachyzoite yield (TY) was recorded in cultures treated with compound 1553. Longer treatments for up to 24 h were more effective but failed to inhibit parasite proliferation completely, not showing statistically significant differences among the compounds. However, TYs diminished to low values after 48 h treatments with all four compounds, and this was corroborated by IFAT. Further analysis by IFAT at 8 and 10 days post treatment showed that tachyzoites remained viable and were able to re-infect host cells even after 48 h post treatment.

Table 3
Percentage of inhibition of parasite growth in the drug screening when bumped kinase inhibitors were administered at 0 or at 6 h p.i. at a concentration of 5 μM.

	Compound	1294	1517	1553	1571	1575	1586	1597	1605	1649
Time of administration	0 h p.i.	99	98	98	96	95	92	95	96	63
	6 h p.i.	90	93	96	95	89	87	83	87	63

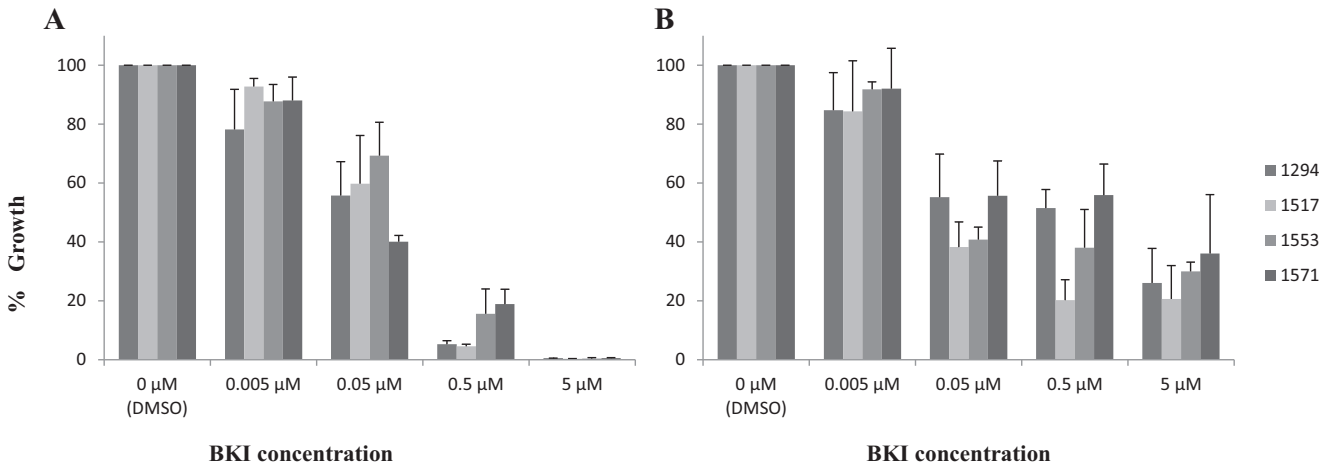

Fig. 2. Percentages of *Besnoitia besnoiti* growth inhibition (related to negative control, dimethyl sulfoxide) when bumped kinase inhibitors are administered at 0 h p.i. (A) and at 24 h p.i. (B) as determined by quantitative real-time PCR. Error bars in graphs represent the S.D.

Table 4
In vitro activity of selected bumped kinase inhibitors against *Besnoitia besnoiti* tachyzoite proliferation (EC_{50} and EC_{99} values (μM)).

Compound	1294	1517	1553	1571
EC_{50} (*B. besnoiti*)	0.045	0.067	0.097	0.051
EC_{99} (*B. besnoiti*)	2.38	2.28	3.35	2.78

Lysis plaques were present in 6 and 24 h treated wells both at 8 and 10 days post treatment, whilst in 48 h treated wells only parasitophorous vacuoles could be found.

3.7. Determination of the effects of BKIs on the ultrastructure of *B. besnoiti* tachyzoites: Transmission Electron Microscopy analysis

In control cultures, which were exposed to solvent but not to drugs, *B. besnoiti* tachyzoites underwent intracellular proliferation within a PV, surrounded by a PV membrane (PVM) (Fig. 4). In longitudinal sections they exhibited the typical features of apicomplexan parasites including a polar organisation, apical organelles such as micronemes and rhoptries, dense granules, nucleus and mitochondrion. Individual tachyzoites were more clearly visible in smaller vacuoles (Fig. 4A, B), and appeared more tightly packed in larger vacuoles (Fig. 4C, D). In the infected HFF cell cultures treated with the four selected BKIs, clear alterations were visible, which were mostly very similar for all four BKIs. As exemplified for BKI-1294 (Fig. 5A–D), a fraction of parasites was evidently distorted, with highly vacuolized cytoplasm and most likely nonviable, while inside the same host cell, still intact parasites formed multinucleated complexes, some of which remained viable for up to 8 days and clearly grew in size (Fig. 5D). These complexes were a large mass that contained several nuclei and apical complex precursors, already containing structural features such as conoids and secretory organelles. However, parasites appeared stuck in the cell cycle and could not complete cytokinesis. BKI-1571 and 1553 also induced the formation of such complexes (Fig. 5E, F), while compound 1517-treated cultures often exhibited already distorted tachyzoites and still viable complexes within the same host cells as shown in Fig. 5H. BKI-treated parasites, in general, often formed amylopectin granules (Fig. 5), which represent a source of energy in apicomplexan bradyzoites. Host cell mitochondria were often unaffected and appeared still intact, suggesting that the host cells were not extensively affected.

Compounds 1294 (Fig. 5A–D) and 1517 (Fig. 5H) showed a more dramatic effect on the ultrastructure of the tachyzoites, seemingly being more lethal with severe alterations in the cytoplasms and membranes of the parasites.

Alterations in the ultra-structure of the tachyzoites and the morphology of the PV were suggested based to IFAT results (Fig. 6). In BKI-treated wells, seemingly distorted PVs with non-discernible tachyzoites were visualised, whilst in DMSO-treated control wells parasitophorous vacuoles showed the characteristic rossetta morphology and zoites were clearly discernible by a surface staining with the antibody employed.

4. Discussion

This study shows that *Bb*CDPK1 could represent a promising drug target for the treatment of bovine besnoitiosis. First, we have shown the transcription of a CDPK1 homologue in *B. besnoiti* tachyzoites, namely *Bb*CDPK1. Next, the activity of recombinant *Bb*CDPK1 was inhibited by a panel of BKIs. Thirdly, selected BKIs were shown to have a profound impact on *B. besnoiti* host cell invasion and proliferation, and these effects were visualised by immunofluorescence and TEM.

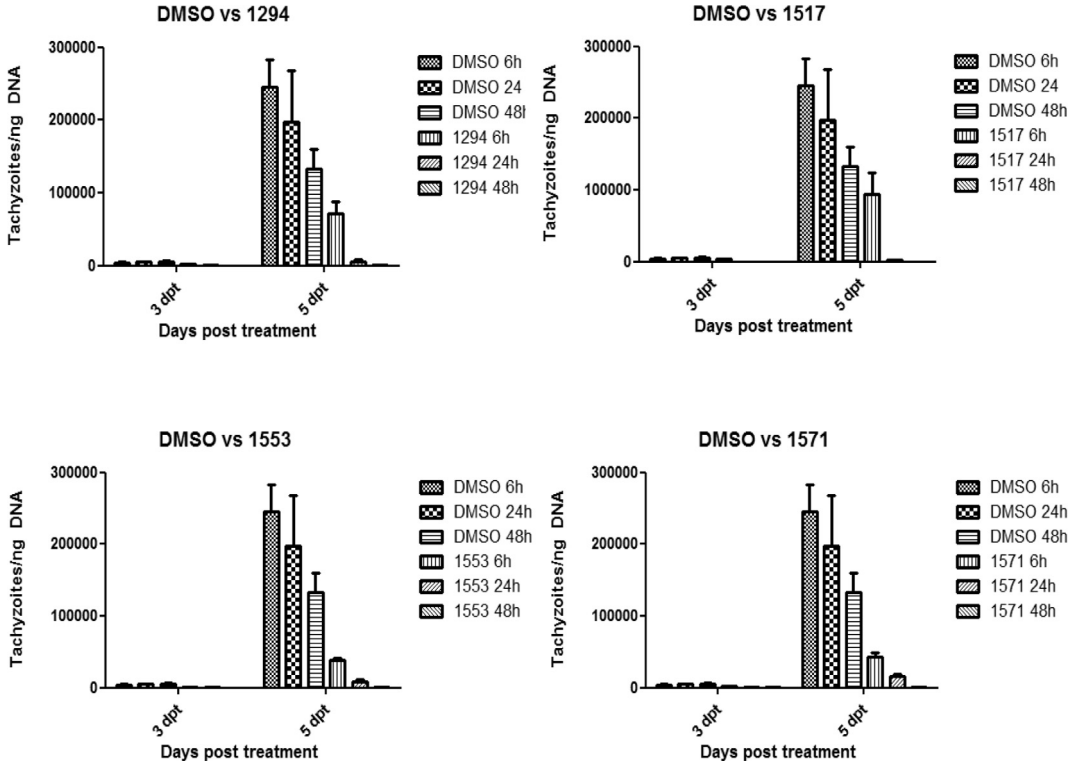

Fig. 3. Tachyzoite yield expressed as tachyzoites per ng of DNA from *Besnoitia besnoiti* cell cultures infected and treated with the four bumped kinase inhibitors selected for 6, 24 or 48 h collected at 3 and 5 days post treatment. Error bars in graphs represent the standard deviation

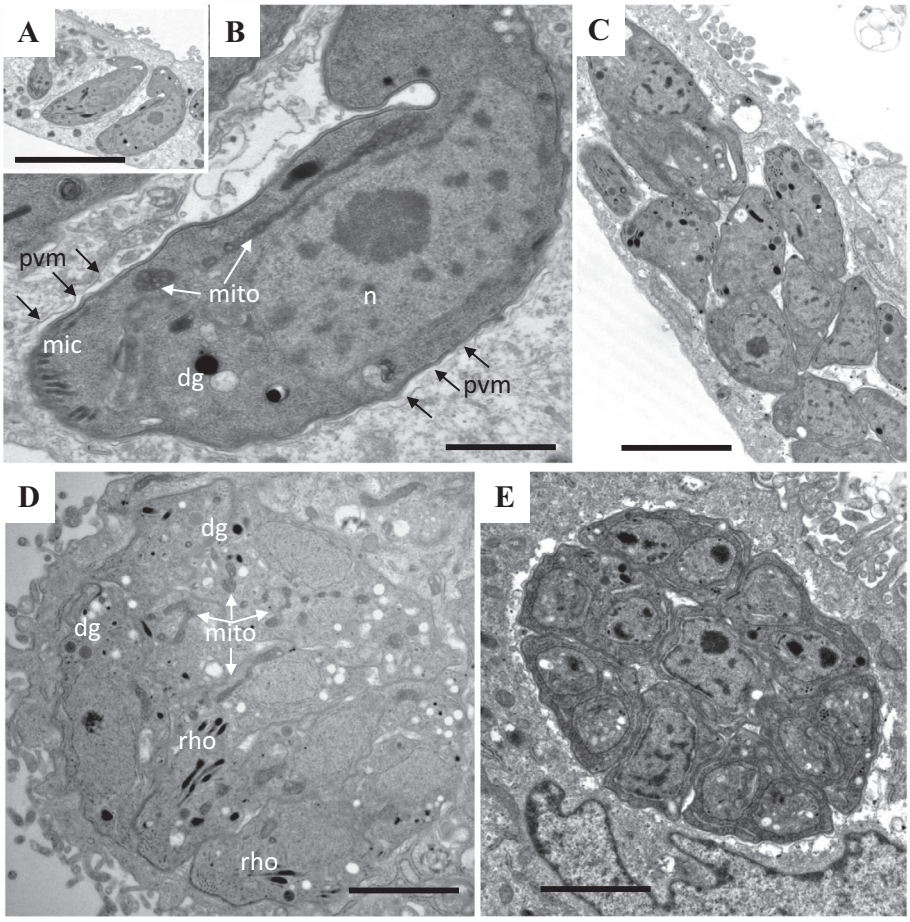

Fig. 4. Representative Transmission Electron Microscopy images of *Besnoitia besnoiti* tachyzoites in human foreskin fibroblast cell cultures treated with DMSO. Intact tachyzoites are observed in longitudinal (A, B, C) and transversal cut sections (C, D, E). Note B is a larger magnification view of A. Numerous viable tachyzoites, located within parasitophorous vacuoles surrounded by a parasitophorous vacuole membrane (A, D, E), can be seen. Non-distorted apical complexes contained typical organelles of apicomplexan parasites, such as the conoid (con), dense granules (dg), micronemes (mic) and rhoptries (rho) (B, D). Also, mitochondria (mito) and the nucleous (nuc) of the tachyzoites are clearly discernible. Scale bars: A = 3 μm; B = 0.5 μm; C = 1.2 μm; D = 1.2 μm; E = 1.2 μm.

As expected, the CDPK1-type kinase identified in *B. besnoiti* showed a high degree of sequence similarities with CDPK1 enzymes from other members of the Toxoplasmatinae (*T. gondii* and *N. caninum*). Indeed, the amino acid sequence of *Bb*CDPK1 reported herein shares a high percentage of identity (95%) with orthologues *Nc*CDPK1 and *Tg*CDPK1, including a glycine in the gatekeeper position, which discriminates CDPK1 from other kinases (Ojo et al., 2014). The sequence showed additional characteristic features of CDPK1 enzymes such as an N-terminal serine-threonine kinase domain, a junctional domain and a series of calcium-binding domains known as EF hands. The existence of EF hands suggest that *Bb*CDPK1 might play an important role in regulating calcium-dependent pathways (Hui et al., 2015). Moreover, the sequence showed the closest structural similarity with *Tg*CDPK1. Accordingly, the newly identified orthologue was named *Bb*CDPK1. Besides, putative n-myristoylation residues were found, similar to what has been reported for *Cryptosporidium Cp*CDPKs (Etzold et al., 2014), which may be important for the association of the enzyme with lipid membranes that can influence its activity.

Kinase assays showed that selected BKIs inhibited the *Bb*CDPK1 enzyme activity even at low nanomolar range concentrations. A similar finding occurred with both *Nc*CDPK1 and *Tg*CDPK1, whose X-ray crystal structures confirmed a structural basis for BKI selectivity (Ojo et al., 2010, 2014). These observations are supported by the high kinase domain sequence identity found in members of the Toxoplasmatinae, where the percentage of identity of *Bb*CDPK1 is as high as 98% and 98.4% with *Tg*CDPK1 and *Nc*CDPK1, respectively. Previously, it has been shown that the degree of sensitivity or resistance of CDPK enzymes to these inhibitors depends on the size and characteristics of the gatekeeper residue and the topology of the adjacent ATP-binding pocket (Keyloun et al., 2014). Regarding this issue, *Bb*CDPK1 possesses only a single amino acid difference in the active site compared with *Tg*CDPK1 and *Nc*CDPK1 sequences (Phenylalanine in position 112 instead of Tyrosine). Consequently, a similar susceptibility pattern against BKIs was expected in all of the Toxoplasmatinae orthologues with the same atypically small glycine gatekeeper residue (Van Voorhis et al., 2017). Enzymatic results indicated that BKIs may be targeting at least *Bb*CDPK1. Similar effects were observed with the four BKIs studied that effectively inhibit other CDPK1 orthologues present in *N. caninum* (Müller et al., 2017), *T. gondii* (Winzer et al., 2015) and *C. parvum* (Castellanos-Gonzalez et al., 2013). Further studies with a parasite line expressing a gatekeeper mutant would be needed to definitively claim that the in vivo phenotype of BKI-treated parasites is solely due to inhibition of *Bb*CDPK1. In the context of these future studies, it should be also verified whether CDPK1 inhibition in vitro is abolished when a large gatekeeper mutant recombinant enzyme is used for the kinase assay.

The results obtained in in vitro assays suggests that *Bb*CDPK1 may be a key regulator during the parasite lytic cycle, since invasion and proliferation events were severely impaired as in *N. caninum* and *T. gondii* (Müller et al., 2017). We included in this panel

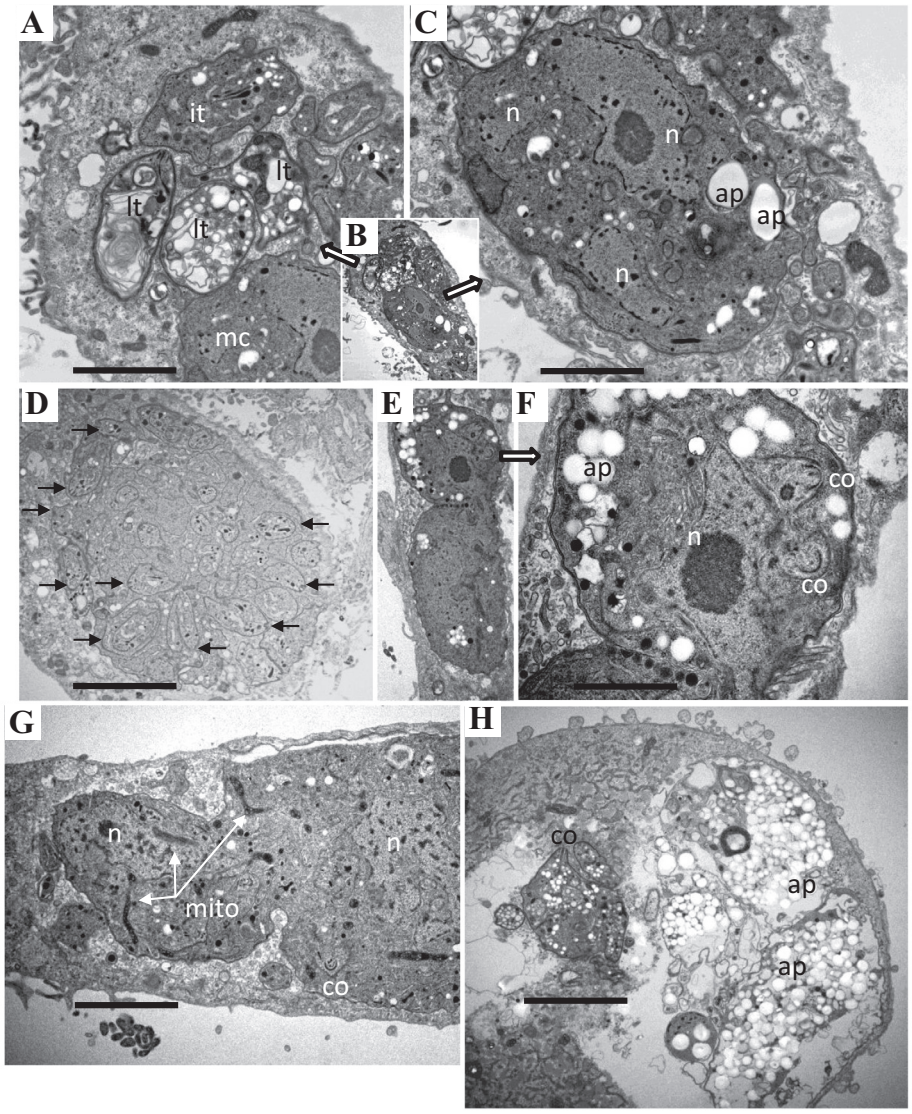

Fig. 5. Representative Transmission Electron Microscopy images of *Besnoitia besnoiti* tachyzoites in human foreskin fibroblast cell cultures treated with bumped kinase inhibitors such as 1294 for 4 days (A–C) or 6 days (D), 1571 for 4 days (E, F), 1553 for 6 days (G) and 1517 for 6 days (H). (A, C) Largely distorted tachyzoites (lt), intact parasites (it) and complexes (mc) can be present in a single host cell. (B) A and C are larger magnification views of B, showing largely distorted and intact tachyzoites (A) or a multinucleated compound (C). A low magnification view. (D) A large complex generated by exposure to bumped kinase inhibitor 1294 for 6 days which contains numerous precursors of apical complexes marked with arrows. (E) A complex exhibiting numerous amylopectin granules (ap); note the two emerging conoids (co). (F) A larger magnification view of E. (G) Exposure to bumped kinase inhibitor 1553 also results in the formation of large complexes; note the intact mitochondria (mito) and emerging conoid structure (co). H: 1517 treatment results in the formation of parasites that form large cytoplasmic amylopectin granule deposits. Scale bars: A = 2 μm, C = 1.6 μm, D = 4.2 μm, F = 1.3 μm; G = 2.8 μm, H = 3.4 μm.

of BKIs the well-studied BKI 1294 which has been used in in vitro and in vivo assays against *Theileria equi* (Hines et al., 2015), *C. parvum* (Lendner et al., 2015), *T. gondii* (Doggett et al., 2014; Winzer et al., 2015) and *N. caninum* (Ojo et al., 2014; Müller et al., 2017), together with other novel and less studied BKIs. Eight out of nine compounds effectively inhibited parasite invasion, with BKIs 1294, 1517, 1553 and 1571 being the most promising ones (inhibition of parasite invasion > 90%) when administered at 5 μM at 0 and at 6 h p.i. Moreover, these compounds lacked cytotoxicity in Marc-145 cells when applied at this concentration, as was also observed by Müller et al. (2017) in human foreskin fibroblast cells.

The EC_{50} and EC_{99} values obtained for these four compounds are in the nanomolar range, which is in accordance with those published for *N. caninum* (Ojo et al., 2014; Müller et al., 2017) and *T. gondii* (Winzer et al., 2015). Most parasite clearance was accomplished by treatments with EC_{99} concentrations only after 72 h of treatment, whereas short treatments did not completely inhibit parasite proliferation, suggesting that these BKIs are parasitostatic rather than parasiticidal. This was confirmed by visualising cultures at 8 and 10 days post treatment, which revealed the presence of remaining viable tachyzoites in drug-treated cultures re-infecting host cells, and by TEM analyses that showed seemingly still viable tachyzoites. TEM showed that the effects of these compounds were not limited to the arrest of host cell invasion, suggesting that there may be additional targets involved (Ojo et al., 2014). Thus, it is possible that secondary targets besides CDPK1 are affected. In *T. gondii* for instance, Mitogen-Activated Protein kinase (MAPK) was previously shown to be inhibited by a BKI analogue, with different pyrazolo-pyrimidine R1 and R2 groups (Sugi et al., 2013, 2015). Inspection of BKI-treated *B. besnoiti* by TEM revealed similar findings for BKIs 1294, 1517, 1553 and 1571. Exposure to these BKIs led to severe ultrastructural alterations in some, but not all, tachyzoites. At later time points after 4–6 days of treatment, PVs containing large multinucleated complexes were found,

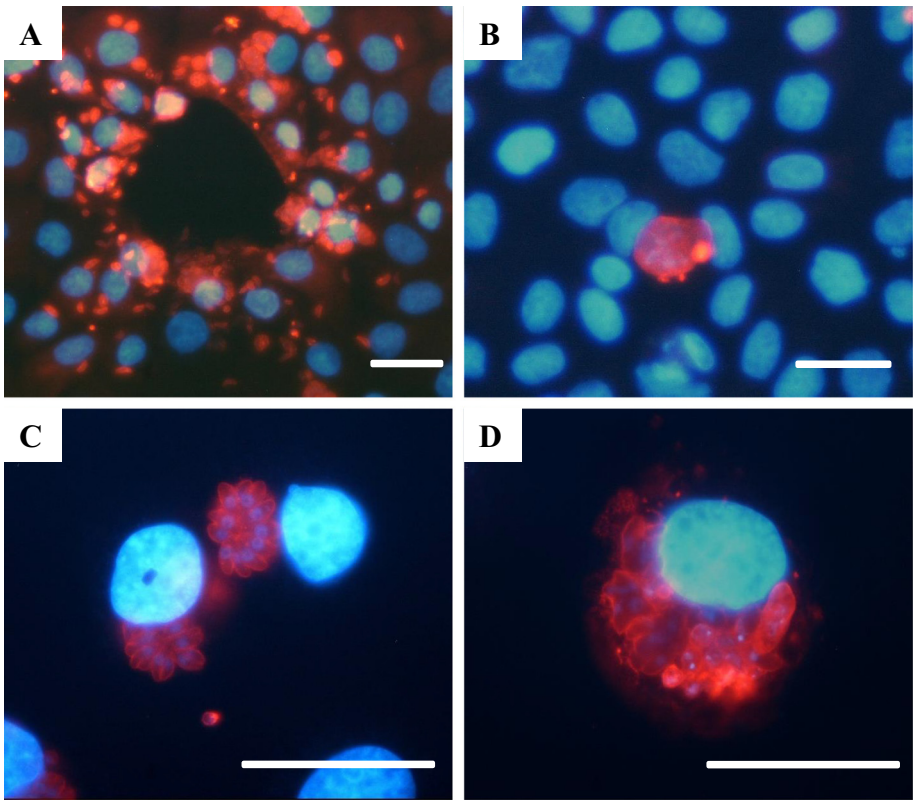

Fig. 6. Marc-145 cell cultures infected with *Besnoitia besnoiti* and treated with DMSO or bumped kinase inhibitor 1294 for 3 days. (A) Marc-145 cell culture infected with *B. besnoiti* tachyzoites and treated with DMSO. Note a lysis plaque. (B) Culture treated with bumped kinase inhibitor 1294 at 5 μM for 3 days. (C) Culture treated with bumped kinase inhibitor 1294 at 0.5 μM for 3 days. Note a seemingly viable parasitophorous vacuole (PV) with well-defined tachyzoites. (D) Culture treated with bumped kinase inhibitor 1294 at 0.5 μM for 3 days. Note a distorted PV with tachyzoites that are not well-defined. Scale bars: A = 40 μm, B = 40 μm, C = 40 μm, D = 40 μm.

some of which showed clear signs of cellular degeneration and others obviously still viable, similar to what has been reported earlier in BKI-1294, 1517 and 1553 treated cell cultures infected with *N. caninum* or *T. gondii* (Winzer et al., 2015; Müller et al., 2017). As for *N. caninum,* BKIs 1294 and 1517 showed more dramatic effects (Müller et al., 2017). These complexes result from parasites that undergo nuclear division, but not cytokinesis, resulting in the formation of tachyzoite precursors that are trapped within the host cell. Whether this effect is due to CDPK1 inhibition or whether there are other targets of BKIs which regulate parasite cytokinesis needs to be elucidated.

In addition, BKI 1294 treatment induced higher expression levels of bradyzoite-specific genes (i.e. MAG1, BAG1) in drug-treated cultures infected with *N. caninum* and *T. gondii,* and increased labelling intensity for anti-BAG1 and anti-CC2 bradyzoite-specific markers was noted (Winzer et al., 2015). Similar increased staining with the bradyzoite marker MAG1 was observed in *N. caninum* tachyzoites treated with BKI 1517 and 1553, together with an increased presence of amylopectin granules as visualised by TEM (Müller et al., 2017). Similarly, amylopectin granules were present in BKI-treated *B. besnoiti*, a characteristic feature of *B. besnoiti* bradyzoites (Fernández-García et al., 2009). This is particularly interesting, since BKI treatments could potentially represent a convenient exogenous trigger to induce tachyzoite-to-bradyzoite conversion of *B. besnoiti* in vitro.

In conclusion, we here demonstrate the therapeutic potential of BKIs for treatment of bovine besnoitiosis. Prospectively, one could envisage BKI treatment of affected cattle at the acute stage of infection where tachyzoites replicate and disseminate, inducing vascular damage and clinical signs of respiratory disorders and orchitis. During the chronic stage, BKI therapy might be more difficult, possibly due to potentially poor drug accessibility to the interior of bradyzoite-containing tissue cysts (Álvarez-García et al., 2014). A major caveat for the development of BKIs against besnoitiosis is the absence of laboratory animal models; thus studies need to be carried out directly in the target animal (Álvarez-García et al., 2014). Plasma levels of up to 5 μM have been already achieved in cattle treated with BKI 1294, 1517 and 1553 (Huang et al., 2015; Schaefer et al., 2016; Hulverson et al., 2017), and whether the administration of these BKIs during the acute stage of the disease is enough to avoid tissue cyst formation needs to be further investigated.

Acknowledgements

This work was financially supported through two research projects from the Spanish Ministry of Economy and Competitiveness (Ref. AGL2013-04442) and Community of Madrid, Spain (Ref. S2013/ABI-2906, PLATESA-CM), and by the Swiss National Science Foundation (grant No. 310030_165782 and CRSII3_160702). We also acknowledge support from the National Institute of Allergy and Infectious Diseases, USA and National Institute of Child Health and Human Development of the National Institutes of Health, USA under the award numbers R01AI089441, R01AI111341, and R01HD080670. The work was also supported by awards # 2014-06183 from the United States Department of Agriculture National Institute of Food and Agriculture. Alejandro Jiménez-Meléndez was supported by a grant from the Spanish Ministry of Education, Culture and Sports (grant n° FPU13/05481). In addition, we acknowledge Laura Jiménez-Pelayo and Marta García-Sánchez for their technical assistance. Conflict of Interest Disclosure: Dr. Van Voorhis is the founder of the company ParaTheraTech Inc., dedicated to bringing BKIs to market in animal health applications. He did not carry out or interpret the experiments in this paper.

Appendix A. Supplementary data

Supplementary data associated with this article can be found, in the online version, at http://dx.doi.org/10.1016/j.ijpara.2017.08.005.

References

Álvarez-García, G., Frey, C.F., Mora, L.M., Schares, G., 2013. A century of bovine besnoitiosis: an unknown disease re-emerging in Europe. Trends Parasitol. 29, 407–415.

Álvarez-García, G., García-Lunar, P., Gutiérrez-Expósito, D., Shkap, V., Ortega-Mora, L.M., 2014. Dynamics of *Besnoitia besnoiti* infection in cattle. Parasitology 141, 1419–1435.

Álvarez-García, G., 2016. From the mainland to Ireland – bovine besnoitiosis and its spread in Europe. Vet. Rec. 178, 605–607.

Arnal, M., Gutiérrez-Expósito, D., Martínez-Durán, D., Regidor-Cerrillo, J., Revilla, M., Fernández-de-Luco, D., Jiménez-Meléndez, A., Ortega-Mora, L.M., Álvarez-García, G., 2017. Systemic besnoitiosis in a juvenile roe deer (*Capreolus capreolus*). Transbound. Emerg. Dis. (in press)

Basso, W., Schares, G., Gollnick, N.S., Rutten, M., Deplazes, P., 2011. Exploring the life cycle of *Besnoitia besnoiti* – experimental infection of putative definitive and intermediate host species. Vet. Parasitol. 178, 223–234.

Billker, O., Lourido, S., Sibley, L.D., 2009. Calcium-dependent signaling and kinases in apicomplexan parasites. Cell Host Microbe 5, 612–622.

Castellanos-Gonzalez, A., White Jr, A.C., Ojo, K.K., Vidadala, R.S., Zhang, Z., Reid, M.C., Fox, A.M., Keyloun, K.R., Rivas, K., Irani, A., Dann, S.M., Fan, E., Maly, D.J., Van Voorhis, W.C., 2013. A novel calcium-dependent protein kinase inhibitor as a lead compound for treating cryptosporidiosis. J. Infect. Dis. 208, 1342–1348.

Cortes, H.C., Muller, N., Esposito, M., Leitao, A., Naguleswaran, A., Hemphill, A., 2007. *In vitro* efficacy of nitro- and bromo-thiazolyl-salicylamide compounds (thiazolides) against *Besnoitia besnoiti* infection in Vero cells. Parasitology 134, 975–985.

Cortes, H.C., Muller, N., Boykin, D., Stephens, C.E., Hemphill, A., 2011. *In vitro* effects of arylimidamides against *Besnoitia besnoiti* infection in Vero cells. Parasitology 138, 583–592.

Diesing, L., Heydorn, A.O., Matuschka, F.R., Bauer, C., Pipano, E., de Waal, D.T., Potgieter, F.T., 1988. *Besnoitia besnoiti*: Studies on the definitive host and experimental infections in cattle. Parasitol. Res. 75, 114–117.

Doerig, C., Meijer, L., Mottram, J.C., 2002. Protein kinases as drug targets in parasitic protozoa. Trends Parasitol. 18, 366–371.

Doggett, J.S., Ojo, K.K., Fan, E., Maly, D.J., Van Voorhis, W.C., 2014. Bumped kinase inhibitor 1294 treats established *Toxoplasma gondii* infection. Antimicrob. Agents Chemother. 58, 3547–3549.

Etzold, M., Lendner, M., Daugschies, A., Dyachenko, V., 2014. CDPKs of *Cryptosporidium parvum*—stage-specific expression *in vitro*. Parasitol. Res. 113, 2525–2533.

EFSA European Food Safety Authority, 2010. Bovine besnoitiosis: an emerging disease in Europe. Scientific statement on bovine besnoitiosis. EFSA J 8, 1499.

Fernández-García, A., Risco-Castillo, V., Pedraza-Díaz, S., Aguado-Martínez, A., Álvarez-García, G., Gómez-Bautista, M., Collantes-Fernández, E., Ortega-Mora, L., 2009a. First isolation of *Besnoitia besnoiti* from a chronically infected cow in Spain. J. Parasitol. 95, 474–476.

Fernández-García, A., Álvarez-García, G., Risco-Castillo, V., Aguado-Martínez, A., Marugán-Hernández, V., Ortega-Mora, L.M., 2009b. Pattern of recognition of *Besnoitia besnoiti* tachyzoite and bradyzoite antigens by naturally infected cattle. Vet. Parasitol. 164, 104–110.

Franc, M., Cardiegues, M., 1999. La besnoitiose bovine: attitude diagnostique et therapeutique. Bulletin des GTV. Bovins, Parasitologie, 119–124.

Frey, C.F., Regidor-Cerrillo, J., Marreros, N., García-Lunar, P., Gutiérrez-Expósito, D., Schares, G., Dubey, J.P., Gentile, A., Jacquiet, P., Shkap, V., Cortes, H., Ortega-Mora, L.M., Álvarez-Garcia, G., 2016. *Besnoitia besnoiti* lytic cycle *in vitro* and differences in invasion and intracellular proliferation among isolates. Parasit. Vectors 9, 1.

Greenbaum, D.C., 2008. Is chemical genetics the new frontier for malaria biology? Trends Pharmacol Sci. 29, 51–56.

Gutiérrez-Expósito, D., Ortega-Mora, L.M., Marco, I., Boadella, M., Gortázar, C., San Miguel-Ayanz, J.M., García-Lunar, P., Lavin, S., Álvarez-García, G., 2013. First serosurvey of *Besnoitia* spp. infection in wild european ruminants in Spain. Vet. Parasitol. 197, 557–564.

Hines, S.A., Ramsay, J.D., Kappmeyer, L.S., Lau, A.O.T., Ojo, K.K., Van Voorhis, W.C., Knowles, D.P., Mealey, R.H., 2015. *Theileria equi* isolates vary in susceptibility to imidocarb dipropionate but demonstrate uniform *in vitro* susceptibility to a bumped kinase inhibitor. Parasit. Vectors 8, 33.

Huang, W., Ojo, K.K., Zhang, Z., Rivas, K., Vidadala, R.S.R., Scheele, S., DeRocher, A.E., Choi, R., Hulverson, M.A., Barrett, L.K., Bruzual, I., Diddaramaiah, L.K., Kerchner, L.M., Kurnick, M.D., Freiberg, G.M., Kempf, D., Hol, W.G., Merrit, E.A., Neckermann, G., de Hostos, E.I., Isoherranen, N., Maly, D.J., Parsons, M., Doggett, J.S., Van Voorhis, W.C., Fan, E., 2015. SAR studies of 5-aminopyrazole-4-carboxamide analogues as potent and selective inhibitors of *Toxoplasma gondii* CDPK1. ACS Med. Chem. Lett. 6, 1184–1189.

Hui, R., El Bakkouri, M., Sibley, L.D., 2015. Designing selective inhibitors for calcium-dependent protein kinases in apicomplexans. Trends Pharmacol. Sci. 36, 452–460.

Hulverson, M.A., Vinayak, S., Choi, R., Schaefer, D.A., Castellanos-Gonzalez, A., Vidadala, R.S.R., Brooks, C.F., Herbert, G.T., Betzer, D.P., Whitman, G.R., Sparks, H. N., Arnold, S.L.M., Rivas, K.L., Barre, L.K., White Jr., A.C., Maly, D.J., Riggs, M.W., Striepen, B., Van Voorhis, W.C.,, Maly, D.J., 2017. Bumped-kinase inhibitors for cryptosporidiosis therapy. J. Infect. Dis. 215, 1275–1284.

Keyloun, K.R., Reid, M.C., Choi, R., Song, Y., Fox, A.M., Hillesland, H.K., Zhang, Z., Vidadala, R., Merritt, E.A., Lau, A.O.T., Maly, D.J., Fan, E., Barrett, L.K., Van Voorhis, W.C., Ojo, K.K., 2014. The gatekeeper residue and beyond: homologous calcium-dependent protein kinases as drug development targets for veterinarian apicomplexa parasites. Parasitology 141, 1499–1509.

Lendner, M., Böttcher, D., Delling, C., Ojo, K.K., Van Voorhis, W.C., Daugschies, A., 2015. A novel CDPK1 inhibitor—a potential treatment for cryptosporidiosis in calves? Parasitol. Res. 114, 335–336.

Lourido, S., Shuman, J., Zhang, C., Shokat, K.M., Hui, R., Sibley, L.D., 2010. Calcium-dependent protein kinase 1 is an essential regulator of exocytosis in *Toxoplasma gondii*. Nature 465, 359–362.

Lourido, S., Moreno, S.N., 2015. The calcium signaling toolkit of the apicomplexan parasites *Toxoplasma gondii* and *Plasmodium* spp. Cell Calcium 57, 186–193.

Müller, J., Aguado-Martínez, A., Balmer, V., Maly, D.J., Fan, E., Ortega-Mora, L.M., Ojo, K.K., Van Voorhis, W.C., Hemphill, A., 2017. Two novel calcium-dependent kinase 1-inhibitors interfere with vertical transmission in mice infected with *Neospora caninum* tachyzoites. Antimicrob. Agents Chemother., 02324–2416

Ojo, K.K., Larson, E.T., Keyloun, K.R., Castaneda, L.J., DeRocher, A.E., Inampudi, K.K., Kim, J.E., Arakaki, T.L., Murphy, R.C., Zhang, L., 2010. *Toxoplasma gondii* calcium-dependent protein kinase 1 is a target for selective kinase inhibitors. Nat. Struct. Mol. Biol. 17, 602–607.

Ojo, K.K., Pfander, C., Mueller, N.R., Burstroem, C., Larson, E.T., Bryan, C.M., Fox, A.M., Reid, M.C., Johnson, S.M., Murphy, R.C., Kennedy, M., Mann, H., Leibly, D.J., Hewitt, S.N., Verlinde, C.L., Kappe, S., Merritt, E.A., Maly, D.J., Billker, O., Van Voorhis, W.C., 2012. Transmission of malaria to mosquitoes blocked by bumped kinase inhibitors. J. Clin. Invest. 122, 2301–2305.

Ojo, K.K., Reid, M.C., Kallur Siddaramaiah, L., Muller, J., Winzer, P., Zhang, Z., Keyloun, K.R., Vidadala, R.S., Merritt, E.A., Hol, W.G., Maly, D.J., Fan, E., Van Voorhis, W.C., Hemphill, A., 2014. *Neospora caninum* calcium-dependent protein kinase 1 is an effective drug target for neosporosis therapy. PLoS One 9, e92929.

Ojo, K.K., Dangoudoubiyam, S., Verma, S.K., Scheele, S., DeRocher, A.E., Yeargan, M., Choi, R., Smith, T.R., Rivas, K.L., Hulverson, M.A., 2016. Selective inhibition of *Sarcocystis neurona* calcium-dependent protein kinase 1 for equine protozoal myeloencephalitis therapy. Int. J. Parasitol. 46, 871–880.

Pedroni, M.J., Vidadala, R.S.R., Choi, R., Keyloun, K.R., Reid, M.C., Murphy, R.C., Barrett, L.K., Van Voorhis, W.C., Maly, D.J., Ojo, K.K., 2016. Bumped kinase inhibitor prohibits egression in *Babesia bovis*. Vet. Parasitol. 215, 22–28.

Pols, J.W., 1960. Studies on bovine besnoitiosis with special reference to the aetiology. Onderstepoort J. Vet. Res. 28, 265–356.

Schaefer, D.A., Betzer, D.P., Smith, K.D., Millman, Z.G., Michalski, H.C., Menchaca, S. E., Zambriski, J.A., Ojo, K.K., Hulverson, M.A., Arnold, S.L., Rivas, K.L., Vidadala, R. S., Huang, W., Barrett, L.K., Maly, D.J., Fan, E., Van Voorhis, W.C., Riggs, M.W., 2016. Novel Bumped Kinase Inhibitors are safe and effective therapeutics in the calf clinical model for cryptosporidiosis. J. Infect. Dis. 214, 1856–1864.

Shkap, V., De Waal, D.T., Potgieter, F.T., 1985. Chemotherapy of experimental *Besnoitia besnoiti* infection in rabbits. Onderstepoort J. Vet. Res. 52, 289.

Shkap, V., Pipano, E., Ungar-Waron, H., 1987. Besnoitia besnoiti: Chemotherapeutic trials in vivo and in vitro. Rev. Elev. Med. Vet. Pays. Trop. 40, 259–264.

Srinivasan, N., Krupa, A., 2005. A genomic perspective of protein kinases in Plasmodium falciparum. Proteins. Struct Funct. Bioinf. 58, 180–189.

Sugi, T., Kobayashi, K., Takemae, H., Gong, H., Ishiwa, A., Murakoshi, F., Recuenco, F. C., Iwanaga, T., Horimoto, T., Akashi, H., 2013. Identification of mutations in TgMAPK1 of *Toxoplasma gondii* conferring resistance to 1NM-PP1. Int. J. Parasitol. Drugs Drug Resist. 3, 93–101.

Sugi, T., Kawazu, S., Horimoto, T., Kato, K., 2015. A single mutation in the gatekeeper residue in TgMAPKL-1 restores the inhibitory effect of a bumped kinase inhibitor on the cell cycle. Int. J. Parasitol. Drugs Drug Resist. 5, 1–8.

Van Voorhis, W.C., Doggett, J.S., Parsons, M., Hulverson, M.A., Choi, R., Arnold, S., Riggs, M.W., Hemphill, A., Howe, D.K., Mealey, R.H., Lau, A.O.T., Merrit, E.A., Maly, D.J., Fan, E., Ojo, K.K., 2017. Extended-spectrum antiprotozoal bumped kinase inhibitors: A review. Exp. Parasitol. 180, 71–83.

Vidadala, R.S.R., Rivas, K.L., Ojo, K.K., Hulverson, M.A., Zambriski, J.A., Bruzual, I., Schultz, T.L., Huang, W., Zhang, Z., Scheele, S., DeRocher, A.E., Choi, R., Barrett, L. K., Siddaramaiah, L.K., Hol, W.G., Fan, E., Merritt, E.A., Parsons, M., Freiberg, G., Marsh, K., Kempf, D.J., Carruthers, V.B., Isoherranen, N., Doggett, J.S., Van Voorhis, W.C., Maly, D.J., 2016. Development of an orally available and central nervous system (CNS) penetrant *Toxoplasma gondii* calcium-dependent protein kinase 1 (tg CDPK1) inhibitor with minimal human ether-a-go-go-related gene (hERG) activity for the treatment of toxoplasmosis. J. Med. Chem. 59, 6531–6546.

Ward, P., Equinet, L., Packer, J., Doerig, C., 2004. Protein kinases of the human malaria parasite *Plasmodium falciparum*: The kinome of a divergent eukaryote. BMC Genomics 5, 79.

Winzer, P., Muller, J., Aguado-Martínez, A., Rahman, M., Balmer, V., Manser, V., Ortega-Mora, L.M., Ojo, K.K., Fan, E., Maly, D.J., Van Voorhis, W.C., Hemphill, A., 2015. *In vitro* and *in vivo* effects of the bumped kinase inhibitor 1294 in the related cyst-forming apicomplexans *Toxoplasma gondii* and *Neospora caninum*. Antimicrob. Agents Chemother. 59, 6361–6374.

Yang, J., Yan, R., Roy, A., Xu, D., Poisson, J., Zhang, Y., 2015. The I-TASSER suite: protein structure and function prediction. Nat. Methods 12, 7–8.